

## Chapter 2

# Experimental Materials and Equipments

### 2.1 Experimental Materials

Specimens, got from Da'anshan coal mine shaft groove of 9th return air roadway roof and floor strata, were used in the experiment. The top and bottom of roadway were mainly sandstone; the coal seam were of semi dark type, granular structure, medium hardness and good coal quality. Coal specimens were cylindrical cores with a diameter of 50 mm and a length of 100 mm. The two end planes of every specimen were parallel within an accuracy of  $\pm 0.05$  mm, and both planes were perpendicular to the longitudinal axis with an accuracy of  $\pm 0.25^\circ$  (according to ISRM testing guidelines).

The Da'anshan coal mine, a typical in situ stressed mine, is located 50 km west of Beijing, China, as shown in Fig. 2.1a. The length of Da'anshan mine field is 9 km, the width is 2–4 km, and the area is 25.5 km<sup>2</sup>. The main geological structure of mine field is the SW-NE synclinal fold. There are many strike and incline faults, contact fracture zones and secondary tectonic features. Some coal seams are separated by a few rock layers, as shown in Fig. 2.1b. The first coal seam, marked as #13, has a thickness varying from 0.77 to 2.53 m. Below the #13 coal seam, the material is comprised of a sandy conglomerate with a thickness varying between 0.1 and 0.2 m. Below the sandy conglomerate lies the #12 coal seam, with a thickness varying from 0.64 to 2.41 m. Below the #12 coal seam lies a layer of siltstone and sandstone with a thickness of 0.65–1.14 m. The #10 coal seam is below the siltstone and sandstone, with a thickness ranging from 0 to 7.41 m. Below the #10 coal seam, there is a layer of siltstone and sandstone with a thickness of 1.35–2.78 m. Below this layer of siltstone and sandstone lies the #9 coal seam with a thickness of 0–4.4 m. The #13, #12 and #10 coal seams have been mined out, but the #9 coal seam was currently being mined using the longwall mining method. All of coal specimens for this work were collected from the #9 coal seam. The measured coal stratum was composed of 56.40% are nauseous shale, 26.18% fine sandstone, 5.81% coal and 11.61% metamorphic rock. The locations of mine

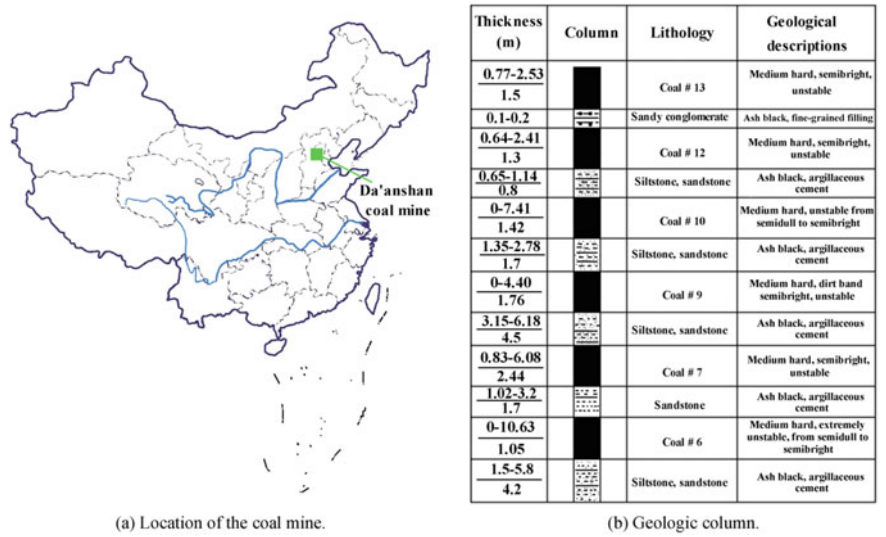


**Fig. 2.1** Location of Da'anshan coal mine and the geologic column of coal seams

and the coal core zones associated with the geological structures in the Da'anshan coal mine are shown in Fig. 2.1.

The rock samples were got from the roof of Xiexhuang mine coal seam, and the roof is mainly limestone. Xiezhuang coal mine is located in the South-West of Xinwen coalfield, 13 km east of Xintai City, mining depth +110 to −1050 m, as shown in Fig. 2.2. The mine is 9–12 km long from east to west and 1.1–4.2 km from north to south, with an area of about 41.5109 km<sup>2</sup>. Geographic coordinates: longitude 117°31'03"–117°41'15", latitude 35°53'45"–35°56'58". East-west length 9–12 km, north-south width of 1.1–4.2 km, an area of about 41.5109 km<sup>2</sup>. Geographic coordinates: longitude 117°31'03"–117°41'15", latitude 35°53'45"–35°56'58". The geological structure of mining area is a northward inclined monoclinic structure, and the subordinate folds are not developed. Coal-bearing strata is a Carboniferous Permian, is toward the east and west, which is a monoclinic structure with a tendency of nearly 6°–36°. It belongs to the Permian Carboniferous land and sea mutual coal deposits in North China. The total thickness of coal seams is 256 m, including 19 coal seams, the average thickness of coal seams is 12.07 m, the total thickness of recoverable coal seams is 10.34 m, and the coal content coefficient is 4%.



**Fig. 2.2** The location of XieZhuang coal mine

## 2.2 Experimental Equipments

### 2.2.1 Laboratory Equipments

#### 1. Servo Stiffness Compressor

The specimens were loaded by a microcomputer-controlled electrohydraulic servo stiffness compressor (GAW-2000, Chaoyang Test Instrument CO., LTD, Changchun, China). As shown in Fig. 2.3, the compressor can perform tensile test, uniaxial compression test and traditional triaxial test. The computer that connected with the compressor directly controlled indenters; host computer recorded the test data accurately and draw the stress-strain curve of samples. These equipments were used to monitor the failure of specimens immediately and dynamically. After the test, the collected stress and strain data were processed and analysed by electrohydraulic servo stiffness compressor, then we obtained the mechanical parameters of rock and the stress-strain curve during loading.

#### 2. AE Monitoring System

The AE monitoring system equipment includes the PCI-2 fully digital AE signal collection, and the analysis system of Physical Acoustics Company (PAC CO.,



**Fig. 2.3** TAW-2000 computer control electro-hydraulic servo rock triaxial testing machine

New Jersey, USA). As shown in Fig. 2.4, the system has 6 collection channels, including sensor, preamplifier, host, and processing softwares to monitor, collect and store AE signal immediately. It displays the dynamic changes of related parameters on the computer monitor connected with it.

The micro sensors, with a frequency of 300 kHz, can obtain AE events information accurately. Because of small size sensor, the perception ability range is narrow. Therefore, it is only suitable for specimens with relatively small scales. The preamplifier has an automatic testing function with a frequency range of 20–1200 kHz, the preamplifier has three different level, 20, 40 and 60 dB respectively, can adapt to different test conditions and requirements. The processing card of AE collection system (PCI-II) is larger range, from 1 kHz to 3 MHz, and has conversion rate of 18 bit A/D. The system has 6 collection channels, which can guarantee the acquisition and processing of signals. Meanwhile, the 6 channels can



**Fig. 2.4** PCI-II AE testing system

also realize the three-dimensional positioning of AE events. The processing software of this system can realize the acquisition and storage of AE signals immediately, and can replay the whole process of AE signal collection, export various AE parameters. AE signal source can also be automatically located by this system (one-dimensional line location, two-dimensional area localization and three-dimensional spatial localization).

### 3. Infrared Thermal Imager

The uncooled infrared focal plane thermal imager (InfRec R300) was used to detect the infrared radiation temperature field of rock samples. This instrument, manufactured by Nec Corp, was a temperature accuracy of 0.05 centigrade, a spatial resolution of 1.2 rad, and a resolution of  $320 \times 240$  pixels. The temperature range of InfRec R300 is from 10 to 40 centigrade, and the highest graphic recording rate was 60 frames per second. The working spectrum of thermal imager cameras ranged from 8 to 14  $\mu\text{m}$ , could measure surface temperatures in the 8–14  $\mu\text{m}$  infrared atmospheric window. The decay of radiation signal received was mildly spread through air in the continuous wave length (8–14 m). Therefore, it has a potential advantage over the accuracy of temperature detection. Thermography data is stored in InfRec R300 in a time series and can be analyzed by the attached NS 9500 software, as shown in Fig. 2.5.

### 3. CT Test Scanning Equipment

As shown in Fig. 2.6, X-ray industrial CT test inspection system (ACTIS300-320/225, Bio-Imaging Research, Inc. Lincolnshire, Lllinois, United States of America).



**Fig. 2.5** InfRec R300 thermal infrared imager

The system has advantages of 3D reconstruction and high precision image acquisition on large size samples. The obtained images using industrial CT with a high energy X-ray source are high density and spatial resolution. The resolution of industrial CT scanning system is  $0.5 \text{ mm} \times 0.35 \text{ mm} \times 1 \text{ mm}$ . The radiation penetrates the surface of rock sample, the different density in the rock sample can be used to distinguish the different substances, and the energy absorbed by different materials is also different. Therefore, images with different shades were displayed centrally on the data acquisition panel behind the rock sample, rock samples were rotated at constant speed, and were collected and scanned continuously. The system was carried out full range data acquisition and continuous scanning of rock samples, 3D model of rock samples was obtained by reconstruction with the software MIMICS. To carry out more detailed post analysis, we need to segment the 3D model into slices and store it as a two-dimensional bin file, and then convert it into a picture format file through MATLAB software programming. The X-ray classification depends on the size and lithology of rock being tested; this system can be applied to nondestructive testing of metal or nonmetal materials with of different densities. The advantages are nondestructive, accurate and intuitive. In addition, for the undisturbed testing scanning of rock and soil engineering materials, the inhomogeneous distribution characteristics of rock materials and their internal structures were obtained from the scanning images, and the three-dimensional structures of rock samples were accurately restored. The samples were non-disturbance test, microscopic physical and mechanical properties of rock were described, such as the change of density distribution; crack size; the rock impurities and distribution etc.



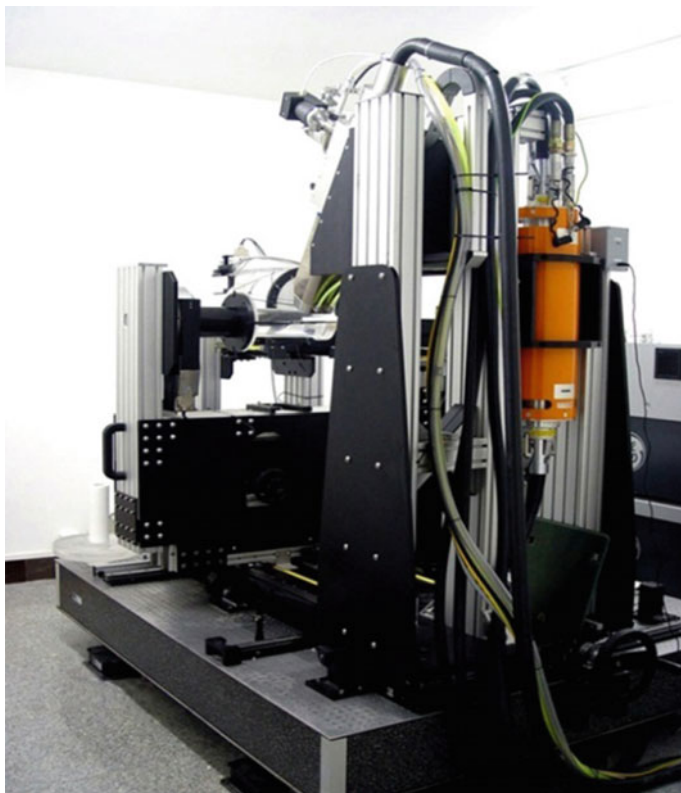


**Fig. 2.6** ACTIS300-320/225 X-ray industrial CT testing system

### **2.2.2 Field Equipment**

Field test equipment is a microseismic monitoring system for Huize Lead-Zinc mine in China. In August 2007, a digital 24-channel MS monitoring system of IMS Company in South African, which consisted of 12 sensors and 4 QS seismic data acquisition instruments, was established to monitor the MS events in deep mining, as shown in Fig. 2.7. Then, the monitoring system was designed, installed, debugged. The monitoring system consists of four parts: surface monitoring station, underground data exchange center, signal acquisitions and sensors. The surface monitoring station was located in the mine pit office building. The underground data exchange center was located in the middle of 1331 m vertical shaft. The sensors were arranged in the surrounding rockmass of monitoring area.

The microseismic monitoring system was divided into two parts: surface and subsurface, they were both long-term monitoring service facilities. The underground data exchange center was located in the 2# shaft portal signal chamber of middle

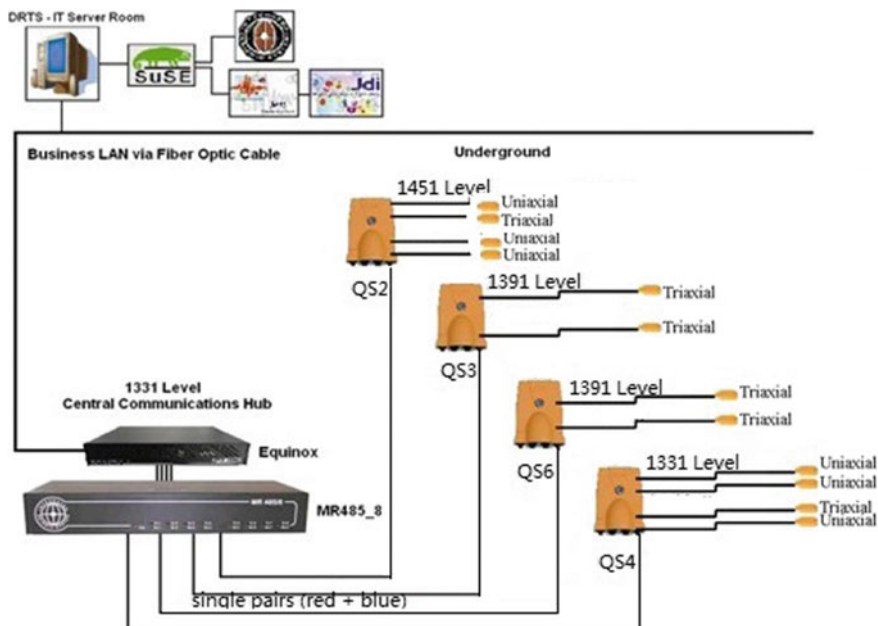


Fig. 2.7 Microseismic monitoring system in Huize mine (after Wang 2013)

section of 1331 m, signal spread to the surface monitoring station through the optical fiber cables, these sensors and the underground data exchanger communicated with the signal cables.

## 2.3 SEM and EDS

Field emission scanning electron microscopy (SEM) is an electronic optical instrument based on modern matter wave theory. In fact, SEM uses a focused high-energy electron beam to observe and scan a sample, thus obtaining a variety of physical information about the samples. Through the acceptance, amplification and display imaging of specific region information of target sample, the surface topography characteristics of sample are observed. Now, this technique has been widely used in micro mechanics research. SEM can be used to observe the metal, ceramics, semiconductors, minerals, and nanoscale one-dimensional, two-dimensional, three-dimensional materials surface and fracture appearance, and the microstructure, size analysis, microstructure and phase distribution of nano-materials. Compared with optical microscopy, scanning electron microscopy has the advantages of simple sample preparation, large depth of field, and wide adjustable range of amplification coefficient, large field of view and high frequency of acquisition.



Energy Dispersive Spectrometer (EDS) is used to analyze component elements, species and their contents of sample, and used in conjunction with scanning electron microscopy and transmission electron microscopy. Since each element has a characteristic wavelength range of X-ray, the energy spectrometer can be used to analyze the composition of material. The spectrometer can be used to analyze the composition and element distribution of Be-U elements of various powders and solid blocks with point, line and surface analysis function, the surface distribution is only 1 min, the scanning speed is quick.

The scanning test was conducted at the Institute of Process Research, Chinese Academy of Sciences. As shown in Fig. 2.8, scanning electron microscope (JSM-7001F) produced by Japan Electronics Corporation and X-MAX energy spectrum analyzer produced by Oxford Instrument Company. The technical parameters are as follows:

- (1) Scanning electron microscope resolution: 2 nm (30 kV)/3.0 nm (1 kV); acceleration voltage: 0.5–30 kV; magnification: 10–500 K.
- (2) The immersion thermal field electron gun has the highest beam intensity of 200 nA, and has the characteristics of large beam and high resolution.
- (3) The automatic diaphragm angle controller does not need to adjust the aperture; fully automatic control of focusing, closing the axis, eliminating astigmatism, and controlling the scanning speed.



**Fig. 2.8** Field emission scanning electron microscope and energy spectrum analyzer

- (4) The design of magnetic leakage is convenient for the observation of magnetic samples, and is suitable for cooperating with a variety of analytical probes.
- (5) The effective area of spectrum probe is  $50 \text{ mm}^2$ , Input count rate  $>500,000 \text{ cps}$ , Acquisition count rate  $>200,000 \text{ cps}$ , the Typical resolution of Mn K  $< 125 \text{ eV}$ , C K $\alpha$   $< 48 \text{ eV}$ .

Figure 2.9 shows SEM images of a sample at magnifications of 200 times, 500 times, 1000 times and 10,000 times. Figure 2.10 depicts the spectrogram, and Table 2.1 shows the chemical composition of samples.

Figure 2.11 shows the SEM image at magnification of 200 times, 1000 times and 2000 times of coal specimens. Figure 2.12 depicts the spectrogram of specimens and Table 2.2 shows the chemical component of coal specimens. It is shown by SEM observation that the coal specimen is a heterogeneous porous material. It is readily found that the rock heterogeneity is attributed to the existence of minerals of different hardness, micro cracks, and micro-cavities.

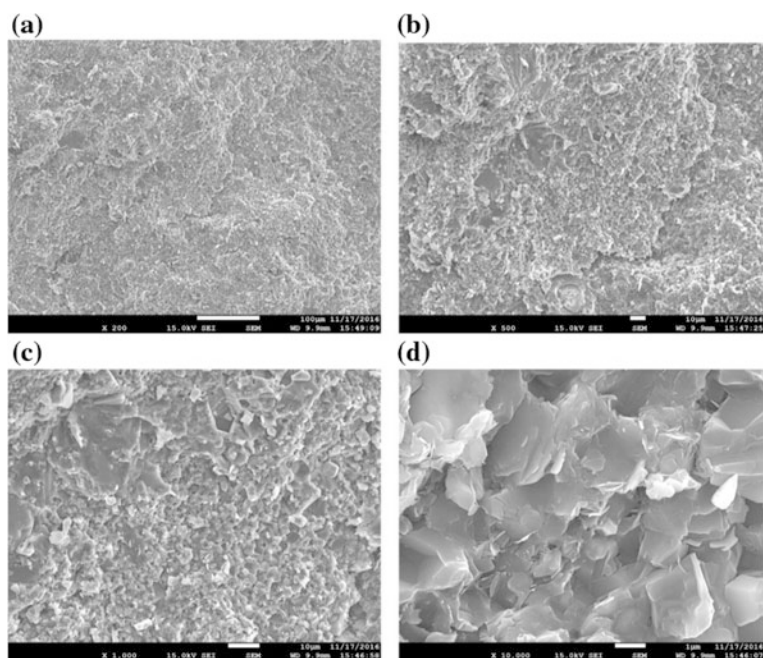


**Fig. 2.9** SEM image at magnification of sample

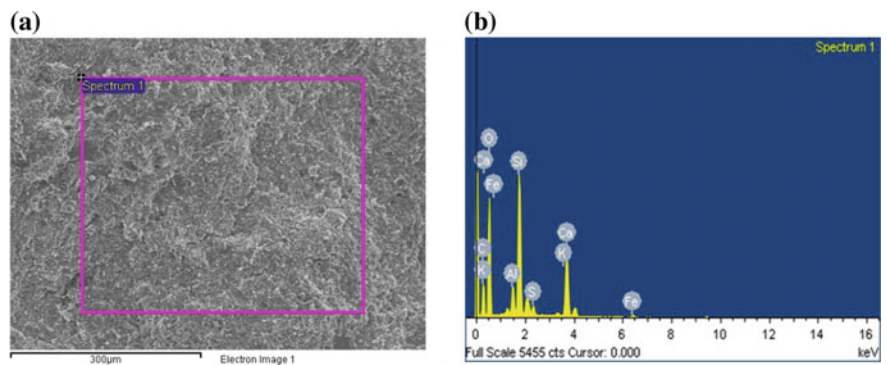


Fig. 2.10 The spectrogram of sample

Table 2.1 Chemical components of samples

Chemical elements	Percentage of weight	Percentage of atoms	Chemical formulas
C	16.86	26.07	CaCO <sub>3</sub>
O	45.84	53.22	SiO <sub>2</sub>
Al	2.59	1.78	Al <sub>2</sub> O <sub>3</sub>
Si	14.67	9.70	SiO <sub>2</sub>
S	1.50	0.87	FeS <sub>2</sub>
K	0.68	0.32	
Ca	15.99	7.41	
Fe	1.87	0.62	Fe

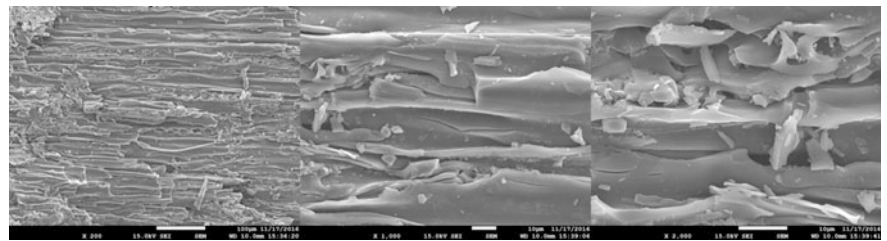


Fig. 2.11 SEM image at magnification of coal specimens

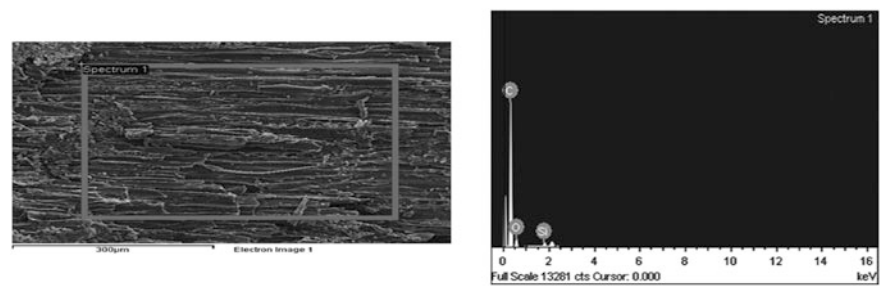


Fig. 2.12 The spectrogram of coal specimens

Table 2.2 Chemical components of coal specimens

Chemical elements	Percentage of weight	Percentage of atoms	Chemical formulas
C K	83.76	87.68	CaCO <sub>3</sub>
O K	14.95	11.75	SiO <sub>2</sub>
Si K	1.28	0.57	SiO <sub>2</sub>

Reference

Wang CL (2013) Identification and early warning method for rock mass instability. Disaster Adv 6 (12):101–105

**Open Access** This chapter is licensed under the terms of the Creative Commons Attribution-NonCommercial 4.0 International License (<http://creativecommons.org/licenses/by-nc/4.0/>), which permits any noncommercial use, sharing, adaptation, distribution and reproduction in any medium or format, as long as you give appropriate credit to the original author(s) and the source, provide a link to the Creative Commons license and indicate if changes were made.

The images or other third party material in this book are included in the book’s Creative Commons license, unless indicated otherwise in a credit line to the material. If material is not included in the book’s Creative Commons license and your intended use is not permitted by statutory regulation or exceeds the permitted use, you will need to obtain permission directly from the copyright holder.



Evolution, Monitoring and Predicting Models of  
Rockburst

Precursor Information for Rock Failure

Wang, C.

2018, XIX, 188 p. 92 illus., 77 illus. in color., Hardcover

ISBN: 978-981-10-7547-6